THE JOURNAL OF BIOLOGICAL CHEMISTRY VOL. 285, NO. 51, pp. 39976–39985, December 17, 2010

A Mouse Macrophage Lipidome*[S]◆

Received for publication, September 8, 2010, and in revised form, October 1, 2010 Published, JBC Papers in Press, October 5, 2010, DOI 10.1074/jbc.M110.182915

Edward A. Dennis,[a,b1,2] Raymond A. Deems,[a] Richard Harkewicz,[b] Oswald Quehenberger,[c] H. Alex Brown,[d1] Stephen B. Milne,[d] David S. Myers,[d] Christopher K. Glass,[c,e1] Gary Hardiman,[c] Donna Reichart,[e] Alfred H. Merrill, Jr.,[f1] M. Cameron Sullards,[f] Elaine Wang,[f] Robert C. Murphy,[g1] Christian R. H. Raetz,[h1] Teresa A. Garrett,[h] Ziqiang Guan,[h] Andrea C. Ryan,[h] David W. Russell,[i1] Jeffrey G. McDonald,[i] Bonne M. Thompson,[i] Walter A. Shaw,[j1] Manish Sud,[k] Yihua Zhao,[k] Shakti Gupta,[k] Mano R. Maurya,[k] Eoin Fahy,[k] and Shankar Subramaniam[a,e,k,l1,3]

From the [a]Department of Chemistry and Biochemistry, [b]Department of Pharmacology, School of Medicine, and [c]Department of Medicine, School of Medicine, University of California, San Diego, La Jolla, California 92093, the [d]Department of Pharmacology, Vanderbilt University School of Medicine, Nashville, Tennessee 37232, the [e]Department of Cellular and Molecular Medicine, School of Medicine, University of California, San Diego, La Jolla, California 92093, the [f]Schools of Biology, Chemistry and Biochemistry and the Petit Institute of Bioengineering and Bioscience, Georgia Institute of Technology, Atlanta, Georgia 30332, the [g]Department of Pharmacology, University of Colorado Denver, Aurora, Colorado 80045, the [h]Department of Biochemistry, Duke University, Medical Center, Durham, North Carolina 27710, the [i]Department of Molecular Genetics, University of Texas Southwestern Medical Center, Dallas, Texas 75390, [j]Avanti Polar Lipids, Inc., Alabaster, Alabama 35007-9105, and the [k]San Diego Supercomputer Center and [l]Department of Bioengineering, University of California, San Diego, La Jolla, California 92093

We report the lipidomic response of the murine macrophage RAW cell line to Kdo_2-lipid A, the active component of an inflammatory lipopolysaccharide functioning as a selective TLR4 agonist and compactin, a statin inhibitor of cholesterol biosynthesis. Analyses of lipid molecular species by dynamic quantitative mass spectrometry and concomitant transcriptomic measurements define the lipidome and demonstrate immediate responses in fatty acid metabolism represented by increases in eicosanoid synthesis and delayed responses characterized by sphingolipid and sterol biosynthesis. Lipid remodeling of glycerolipids, glycerophospholipids, and prenols also take place, indicating that activation of the innate immune system by inflammatory mediators leads to alterations in a majority of mammalian lipid categories, including unanticipated effects of a statin drug. Our studies provide a systems-level view of lipid metabolism and reveal significant connections between lipid and cell signaling and biochemical pathways that contribute to innate immune responses and to pharmacological perturbations.

The "omics" revolution has provided significant insight into the genes, mRNAs, and proteins of mammalian cells, biological systems, and disease (1–3). An important function of these macromolecular classes is the production of metabolites that in turn are used by cells for replication and function. Lipids comprise major structural and metabolic components of cells and have essential functions in the formation of membranes, energy production, and intracellular signaling. Despite the central role of lipids in mammalian cell function, there has been no systematic effort to define the lipid "parts list" of a mammalian cell or the changes in these lipids associated with cellular function and disease. Many biochemical pathways leading to the synthesis and degradation of major lipid categories are known, but how these pathways interact under normal and pathological conditions remains unexplored. Recent advances in mass spectrometry have made it possible to qualitatively and quantitatively analyze a majority of cellular lipids (4–8). We report here a comprehensive systems-level analysis of a mammalian cell lipidome through temporal measurements.

We characterized lipidomic responses of RAW264.7 (RAW) macrophages to a highly specific ligand for Toll-like receptor 4 (TLR4)[4] that mimics aspects of bacterial infection. This model is of particular interest because of the essential roles that alterations in macrophage lipid metabolism play in innate and adaptive immune responses and the development of chronic inflammatory and cardiovascular diseases. Recent studies further suggest that TLR signaling in macrophages is not only required for innate immunity against viral and bacterial pathogens but also contributes to the pathogenesis of atherosclerosis, diabetes, arthritis, and other inflammatory diseases (9). Although TLR4 signaling is known to exert profound effects on the macrophage transcriptome (10), proteome (11), and selected lipid species that underlie protective and pathological functions of the macrophage, the relationships between gene expression changes and global changes in lipid metabolism are largely unknown. By monitoring quantitatively the changes in the major lipids during the temporal response of murine macrophages to an inflammatory stimulus and by integrating the results from these measurements with changes in the

* This work was supported, in whole or in part, by National Institutes of Health Grant through the NIGMS Large Scale Collaborative "Glue" Grant U54 GM069338 (to E. A. D.).

◆ This article was selected as a Paper of the Week.

[S] The on-line version of this article (available at http://www.jbc.org) contains supplemental text, Tables 1–3, and Figs. 1–9.

[1] LIPID MAPS Core Director.

[2] To whom correspondence may be addressed: University of California, San Diego, 9500 Gilman Dr., La Jolla, CA 92093-0601. Tel.: 858-534-3055; E-mail: edennis@ucsd.edu.

[3] To whom correspondence may be addressed: University of California, San Diego, 9500 Gilman Dr., La Jolla, CA 92093-0412. Tel.: 858-822-3625; E-mail: shankar@ucsd.edu.

[4] The abbreviations used are: TLR, Toll-like receptor; KLA, Kdo_2-lipid A; qPCR, quantitative PCR; LXR, liver X receptor; Cer, ceramide; PG, prostaglandin.

macrophage transcriptome at comparable time points, we vastly expand our knowledge of the macrophage lipidome and how it responds to an inflammatory stimulus. We also study a pharmacological perturbation with compactin, an inhibitor of cholesterol biosynthesis, in combination with the inflammatory stimulus so as to assess the amelioration of the inflammatory lipid stimulus by the statin drug. Lipid measurements after KLA/compactin treatment show the expected reduction in sterol biosynthesis and a surprising result, that of increase in some prostaglandins.

MATERIALS AND METHODS

Sample Preparation—RAW264.7 cells were grown in individual core laboratories or centrally and treated for varying periods of time (0–24 h) with Kdo_2-lipid A (KLA) and/or compactin using protocols[5,6] available in the Protocols section of the LIPID MAPS website. To account for biological variability of cells grown in culture and to enhance the statistical power of data analysis, triplicate dishes of cells (technical triplicates) for three independent biological experiments were generally analyzed. Six lipidomics core laboratories located at different institutions developed unique liquid chromatography-mass spectrometric protocols to resolve and quantify the major lipid species in each of the six predominant mammalian lipid categories (12, 13). All lipidomics data (measurements for individual replicates in each lipid category) are available for download from the LIPID MAPS web site (KLA time course and KLA/compactin time course). Lipid measurements are expressed as pmol/μg of DNA, and DNA measurements were conducted as described in the Protocols section of the LIPID MAPS website[7]. The above mentioned website also provides tabular and graphical summaries for each measured analyte as well as statistical analysis in the form of S.E. displayed on time course plots and analysis of variance *p* values for time, treatment (KLA, compactin), and replicate effects. All MS methods (with the exception of fatty acyl-CoA methods) are available for download from the LIPID MAPS website.[8] Extraction conditions, LC-MS protocols, and internal standards were optimized for each lipid category as described in detail elsewhere (14).

Fatty acids, Eicosanoids, and Fatty Acyl-CoA—Eicosanoids and fatty acids were detected and quantitated by mass spectrometric methods (14). Measurements correspond to the intensity of each analyte divided by the intensity of the corresponding deuterated internal standard. The amount of internal standard added to each sample in the time series and control experiments was identical. The relative intensity values were converted to pmol by extrapolating from the standard curve for that analyte and then normalized to the number of cells in a given sample as measured by the quantity of DNA in the well. Fatty acyl-CoAs were detected and quantitated by mass spectrometric methods (14). Measurements correspond to the intensity of each species divided by the intensity of an appropriate internal standard (odd-chain length fatty acyl-CoAs). The amount of internal standard added to each sample in the time series and control experiments was identical. The relative intensity values were converted to pmol and then normalized to the measured quantity of DNA present in each RAW cell preparation following treatment with and without KLA for each time point.

Glycerolipids—Glycerolipids (triacylglycerols, diacylglycerols, and monoether diacylglycerols) were detected and quantitated by mass spectrometric methods (14). Measurements correspond to the abundance of each $[M+NH4]^+$ ion measured as a neutral loss for a specific fatty acid (+NH3) divided by the signal from the d5-labeled internal standard containing that specific fatty acid, obtained in the same neutral loss scan. The amount of internal standard added to each sample in the time series and control experiments was identical. The ratio of these ion abundances was then normalized to the measured quantity of DNA present in each RAW cell preparation following treatment with and without KLA/compactin for each time point.

Glycerophospholipids—Glycerophospholipids (excluding cardiolipins) were detected and quantitated by mass spectrometric methods (14). Measurements in Fig. 4 and supplemental material correspond to the intensity of each species divided by the average intensity (peak area) of a set of odd-chain internal standards corresponding to that particular headgroup. No internal standards were available for the PI series, so the intensity of each species was divided by the total PI intensity in this case. The amount of internal standard added to each sample in the time series and control experiments was identical. The relative intensity values were then normalized to the measured quantity of DNA present in each RAW cell preparation following treatment with and without KLA/compactin for each time point. Cardiolipins were detected and quantitated by mass spectrometric methods (14). The analyte concentration was calculated relative to known amounts of three internal standards of varying fatty acid chain lengths. Within a triplicate sample run, the peak areas of each internal standard were used to calculate a response plot relative to molecular weight. Due to significant overlap of the doubly charged cardiolipin analytes with other singly charged lipids, the first ^{13}C isotope of each analyte was used to extrapolate a relative peak area of the analyte to the internal standard. The contributions of overlapping ^{13}C isotope peaks from species with additional double bonds in the acyl chains were subtracted. The absolute amount of analyte in the sample was calculated by correcting the relative peak area ratios for response based on molecular weights. The absolute amount was normalized for the quantity of DNA in the respective sample well to correct for intersample variations in the number of cells.

Sphingolipids—Sphingolipids were detected and quantitated by mass spectrometric methods (14). Measurements correspond to the intensity of each species divided by the intensity of an appropriate internal standard (C12 analogs for ceramide, glucosylceramide, and sphingomyelin; C20 analogs for sphingosine and sphinganine; C17 analogs for sphingosine-P and sphinganine-P). The amount of internal standard added to each sample in the time series and control experiments was 500 pmol for Cer, GlcCer, and sphingomyelin and 50 pmol for the sphingoid bases (sphingosine and sphinganine, for sphingosine-P

[5] C. K. Glass and D. Reichart, unpublished material.
[6] D. W Russell and B. M. Thompson, unpublished material.
[7] C. K. Glass and D. Reichart, unpublished material.
[8] H. A. Brown, unpublished material.

and sphinganine-P). The relative intensity values were converted to pmol and then normalized to the measured quantity of DNA present in each RAW cell preparation following treatment with and without KLA/compactin for each time point.

Coenzyme Qs and Dolichols—Coenzyme Qs and dolichols were detected and quantitated by mass spectrometric methods (14). The coenzyme Q analyte concentrations were calculated relative to a known amount of coenzyme Q6 internal standard that was spiked into each sample. The absolute amount of analyte in the sample was calculated using the relative peak area of the analyte to the internal standard. The absolute amount was normalized for the quantity of DNA in the respective sample well to correct for intersample variations in the number of cells. The dolichol concentrations were calculated relative to a known amount of the respective nor-dolichol internal standard that was spiked into each sample. The absolute amount of analyte in the sample was calculated using the relative peak area of the analyte to the internal standard. The absolute amount was normalized for the quantity of DNA in the respective sample well to correct for intersample variation in the number of cells.

Sterols and Cholesteryl Esters—Sterols were detected and quantitated by mass spectrometric methods (14). Measurements correspond to pmol amounts of each species, which were determined by dividing the areas under the LC MS/MS elution curve for each species by that for an appropriate deuterated surrogate standard and then multiplying by the amount of the surrogate standard added (~10 pmol to 2 nmol depending on the compound of interest). For most of the analytes, the intensities were similar for equivalent amounts of the analyte as for the internal standard when the LC MS/MS parameters were optimized, and quantitative analysis was conducted by multiple reaction monitoring. If necessary, small corrections were made using empirically determined relative response factors. The pmol amounts were then normalized to the measured quantity of DNA present in each sample (*i.e.* dish of RAW cells at time 0 or at varying times following treatment with and without KLA/compactin). Cholesteryl esters were detected and quantitated by mass spectrometric methods (14). In HPLC/MS/MS measurements by multiple reaction monitoring, the response ratio for each analyte was determined relative to a known amount of internal standard (400 pmol of ^{13}C18 (18:1) cholesteryl ester) that was added to each biological and calibration sample. The absolute amount of each analyte in a sample was then calculated by comparison with a standard curve for a given analyte. Specific six-point calibration curves from 0.0 to 1.6 nmol were constructed for each set of samples for the following cholesterol esters: 14:0, 16:0, 16:1, 18:0, 18:1, 18:2, 20:0, 20:1, 20:2, 20:3, 20:4, and 22:6. Analytes for which no direct reference standard was available were determined based on the curve for a standard closest in number of carbon atoms and double bonds. The reported values were finally adjusted for the amount of DNA measured for each sample.

Microarray Analysis—Microarray analysis was used to measure gene expression response in RAW264.7 cells over time. RAW264.7 cells were harvested at 0.5, 1.0, 2.0, 4.0, 8.0, 12.0, and 24 h after treatment with KLA and/or compactin. At each time point, a custom Agilent array was hybridized, with KLA and/or compactin on the green channel and the control on the red channel. One biological replicate was also run with KLA on the red channel, and the control was run on the green channel (*i.e.* dye-swapped). We evaluated the data and found no dye effects (data not shown). Cells were treated as described in LIPID MAPS protocols.[5,6] The custom Agilent arrays contained 38,489 unique probes for mouse sequences and 21,291 unique mouse genes with Entrez Gene identifiers. Data normalization was performed using the Lowess method. The entire microarray dataset is available online at the LIPID MAPS website and may be searched by multiple criteria including gene symbol, annotation, Entrez gene ID, lipid-related category, and Kyoto Encyclopedia of Genes and Genomes (KEGG) pathway.

Statistical and Other Data and Pathway Analyses—Statistical analysis to identify significantly altered genes and pathways was performed using the VAMPIRE/GOby method and a similar method called cyber-T, which is described in more detail in the supplemental material. Pearson correlation coefficients were calculated for all gene pairs in the dataset. Pearson correlation between lipids and lipid-pathway related genes were computed for each lipid pathway as described in more detail in the supplemental material ("Correlation Analysis" and "Display of the Data and Correlations"). These statistical data are available for viewing and download at the LIPID MAPS website.

Several other types of data analyses were performed and are summarized here. Multiple-way analysis of variance analysis was performed to find the differential effect of KLA, compactin, and time for all genes and lipids. VAMPIRE/cyber-T/GOby analysis was performed to identify which genes are differentially regulated (with respect to control, upon treatment with KLA or compactin, or both) and to find KEGG pathways that are enriched (supplemental material, "Bioinformatics and Statistical Analysis of Microarray Data"). Correlation between qPCR data and microarray data for a select number of genes (15) was analyzed to assess that the microarray data correlate well with actual mRNA levels for most of the important genes in different lipid pathways. The qPCR measurements were calculated as ratios relative to a standard housekeeping gene glyceraldehyde-3-phosphate dehydrogenase (GAPDH) for mRNA samples treated for 8 or 24 h with KLA, compactin, or KLA + compactin or neither (control). Total RNA was isolated from the RAW264.7 cells using the RNeasy mini kit (Qiagen) and DNase I (Invitrogen). First strand cDNA was synthesized using SuperScript 111 and random hexamers (Invitrogen). Samples were run in 20-μl reactions using an AB1 7300 (Applied Biosystems, Foster City, CA). SYBR Green oligonucleotides were used for detection and quantification of a given gene, expressed as relative mRNA level when compared with control, and calculated after normalization to GAPDH using the $\Delta\Delta$ CT method as described by the manufacturer Invitrogen. Weighted Pearson correlation analysis was performed in three ways: 1) among lipids in each individual pathway, 2) among all genes in select KEGG pathways or a LIPID MAPS curated gene list, and 3) between lipids and genes in lipid pathways accounting for time delay for gene translation into proteins (supplemental material, "Correlation Analysis" and "Display of the Data and Correlations"). Weighted correlation-based hierarchical clustering and cluster identification were carried out in

each of the above three cases for each pathway (supplemental material, "Display of the Data and Correlations").

RESULTS AND DISCUSSION

Lipidomic Cascades in Macrophage Cells—RAW macrophage cells were treated with KLA (15), a chemically defined substructure of lipopolysaccharide (LPS), the bacterial molecule that specifically binds to the MD2 subunit of the TLR4 receptor and induces an inflammatory response in macrophages (16). Transcriptional data were quantitatively determined as a function of time by the genomics core employing RNA microarray chips to analyze over 20,000 genes (14). Six lipidomics core laboratories located at different institutions developed unique liquid chromatography-mass spectrometric protocols (14) to resolve and quantify the major lipid molecular species as a function of time in their specific mammalian lipid category (12, 13). A vital aspect of identification and quantification involved the synthesis by the synthetic core of hundreds of chemically pure and often deuterated or odd-chain carbon-containing standards representative of abundant lipids in each of the categories to be analyzed (14); these are now available through Avanti Polar Lipids. Mass spectrometric and transcriptional data collected by the core laboratories were organized using a custom laboratory information management system and transferred to the bioinformatics core for compilation, analysis, and integration (17).

To study the influence of alterations in specific lipid pathways on the response of the macrophages to an inflammatory stimulus, RAW cells were also subjected to a pharmacological perturbation in conjunction with KLA treatment. The statin drug, compactin, demonstrates the expected alterations in the sterol pathway but also affects other inflammatory responses in a systemic manner. These effects bring to focus cross-talk between lipid pathways in inflammation and the metabolic syndrome.

It is now apparent that the lipidome is comprised of hundreds of thousands of unique molecular species of lipids and that metabolism in a given mammalian cell involves many thousands of these. In this initial attempt to define the mammalian lipidome, we have focused on identifying over 400 major lipid molecular species that show dynamic changes in response to an inflammatory response and/or a statin drug, rather than just identifying all species that exist. A global overview of the changes in the murine macrophage lipidome upon KLA treatment is illustrated in Fig. 1, which depicts the interrelationships among major lipid categories, the number of species within each category that were analyzed and changes quantified, and an overall view of the time course of these changes. Catabolism of carbohydrates, proteins, and lipids leads to the production of acetyl CoA, which in turn is converted into fatty acids, sterols, and other intermediary metabolites in the six major lipid categories. Fatty acids (including their CoA and enzyme-bound thioesters) are converted into bioactive eicosanoids and more complex lipids such as glycerolipids (central to energy storage and metabolism), glycerophospholipids, and sphingolipids. The latter two lipid categories are crucial for membrane structure and function, as are the sterols. Sterol esters play key storage and precursor roles within the cell. The transcriptional changes after treatment increased as a function of time with the maximal changes occurring at the 16-h time point. Genes coding for proteins in several lipid metabolic pathways were differentially expressed and were found to correlate significantly with the corresponding metabolite changes. Statistical analysis of lipid changes and concomitant changes in genes associated with lipid pathways are presented in the form of heat maps in supplemental Fig. 1. Comparison of both lipid and gene changes shows that compactin treatment by itself has little effect, except for changes in sterols and sterol genes. KLA treatment with and without compactin shows similar effects with changes in sterols and eicosanoids. We also present changes in lipid transporter genes to depict changes in sterol transporter genes upon KLA-compactin treatment. We carried out quantitative PCR experiments for a number of genes; the correlations between the DNA microarray and qPCR results are presented as a scatterplot in supplemental Fig. 2*A*, and individual qPCR results are presented in supplemental Fig. 2*B*. The lipid metabolic changes in individual lipid categories, the total lipid remodeling strategy employed by the RAW cells, and the effect of an important pharmacological perturbation by a statin drug are discussed below.

Fatty Acids and Fatty Acyls—Activation of phospholipase A_2 to release arachidonic acid for subsequent metabolism is a hallmark of inflammation. The expression of many genes in the arachidonate oxidation pathway increased over time (Fig. 2), with the notable exception of Group IVA phospholipase A_2 (PLA_2), which is activated at the posttranscriptional level (18). As one example of these changes, the cyclooxygenase-2 (COX2) mRNA increased 10-fold at 30 min after KLA treatment. Because the prostaglandin H synthase activity of the COX enzymes is the rate-limiting step in prostaglandin biosynthesis, this increase represents an important component of the inflammatory response. Free arachidonic acid was increased 3-fold after 30 min of stimulation but decreased thereafter (19). This loss can be explained in part by increased COX2 activity and the subsequent enzymatic conversion of arachidonic acid to prostaglandins. Several metabolites arising from the pathway are detected in the cell media, including COX-derived $PGF_{2\alpha}$, PGE_2, and PGD_2, as well as the PGD_2 dehydration metabolites PGJ_2, 15-deoxy-Δ12,14-PGD_2, and 15-deoxy-Δ12,14-PGJ_2 increased with KLA stimulation. 11(*R*)-Hydroxyeicosatetraenoic acid *(11(R)HETE)* (confirmed using chiral chromatography), sometimes arising as a COX product resulting from the arachidonic acid (*AA*) to PGG_2 pathway terminating before completion, was also observed, whereas a number of other potential eicosanoids were not observed as reviewed (20). Toward more advanced analysis of the joint changes in these lipids and the genes/enzymes involved in their biosynthesis, a weighted correlation analysis has been carried out (see supplemental material, "Correlation Analysis" and "Display of the Data and Correlations"). The heat maps of the correlation and data organized according to weighted correlation-based hierarchical clustering are shown in supplemental Fig. 3, *A* and *B*, *top left panel*, (treatment with KLA). In these heat maps, the prostaglandin lipids (*e.g.* PGE_2, PGJ_2, and $PGF_{2\alpha}$) and the prostaglandin synthase genes (Ptgs2, Ptges) change in a similar man-

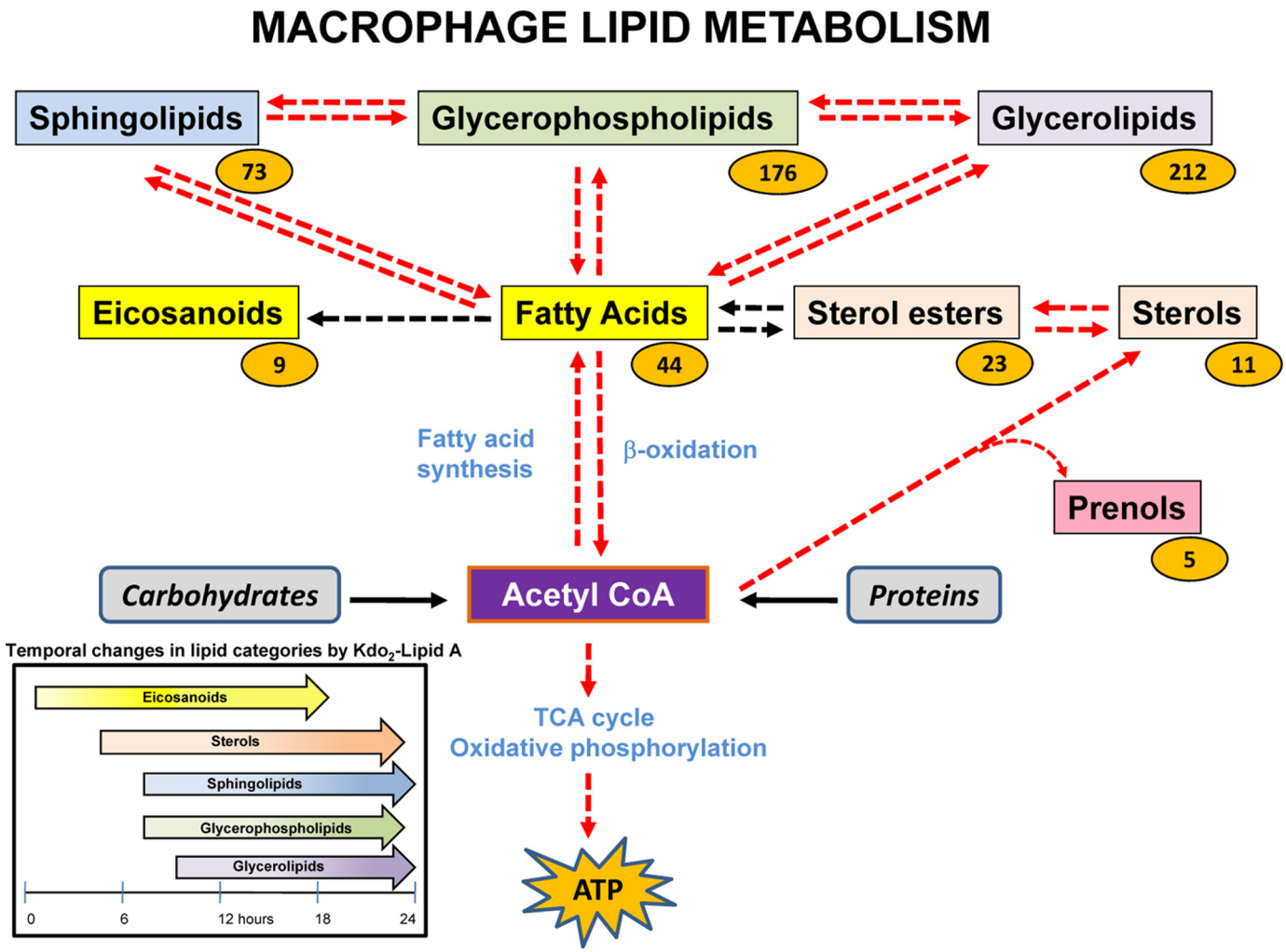

FIGURE 1. **Interrelationships between cellular metabolic pathways.** *Red arrows* denote multistep transformations among the major lipid categories and acetyl CoA. *Black arrows* from fatty acids to sterol esters indicate transfer of fatty acids (in the form of acyl-CoAs) to sterol cores. Values in *orange ovals* represent the number of analytes within each lipid category that were quantified by mass spectrometry in RAW cells in response to stimuli (see under "Results"). The panel at the *lower left* shows a temporal profile of quantitative changes that occur for some lipid species in the various lipid categories in these cells over a 24-h period upon treatment with KLA. The *horizontal arrows* denote the time periods during which statistically significant changes with KLA treatment were observed.

ner, resulting in strong correlation between them (supplemental Table 1, Cluster 2).

Additional fatty acids and fatty acyl-CoAs changed in response to KLA stimulation in RAW cells. Levels of most unsaturated free fatty acids were reduced at longer time points (supplemental Fig. 4*A*), whereas most free saturated fatty acids increased (supplemental Fig. 4*B*). In agreement with these changes, multiple genes encoding fatty acid elongases and desaturases were down-regulated upon treatment. The CoA thioesters of fatty acids were also analyzed (supplemental Fig. 4, *A* and *B*), and many of the monounsaturated species of fatty acyl-CoAs were significantly reduced after 1 h of KLA treatment. (see supplemental Fig. 5 for comparisons between saturated and monounsaturated fatty acyl-CoA responses to KLA). These decreases correlated with a lowered transcript abundance of stearoyl-CoA desaturases 1 and 2 (Entrez Gene IDs 20249 and 20250), which convert 16:0- and 18:0-CoAs to 16:1(9Z)- and 18:1(9Z)-CoA (21), and which in turn are elongated to other monounsaturated fatty acyl-CoAs. Free fatty acid levels are of course also related to the activity of acyl transferases, which remodel them into complex lipids (see below).

Sterols and Prenols—Over a 24-h period of stimulation, intracellular cholesterol levels doubled in treated cells, and the amounts of two intermediates in the cholesterol biosynthetic pathway, lanosterol and desmosterol, increased by 8- and 4-fold, respectively (Fig. 3). Modest increases (2–3-fold) in two oxysterols, 24,25-epoxy-cholesterol and 25-hydroxycholesterol, were observed, and in the latter case, correlated with a 4-fold increase in cholesterol 25-hydroxylase mRNA. The 25-hydroxycholesterol finding was extended to primary macrophages (thioglycolate-elicited, 55-fold increase; bone marrow-derived, 15-fold increase) (data not shown). The expression of genes encoding most of the sterol biosynthetic enzymes decreased over time, with the notable exception of HMG CoA reductase, the rate-limiting enzyme in the pathway. This gene is subject to multiple regulatory inputs (22), one of which may be dominant over signals arising from TLR4 activation. Whether the changes observed in desmosterol, lanosterol, and cholesterol arose from alterations in *de novo* synthesis *versus* the metabolism of cholesterol-rich lipoproteins present in the cell medium was answered in the pharmacological perturbation experiments described below.

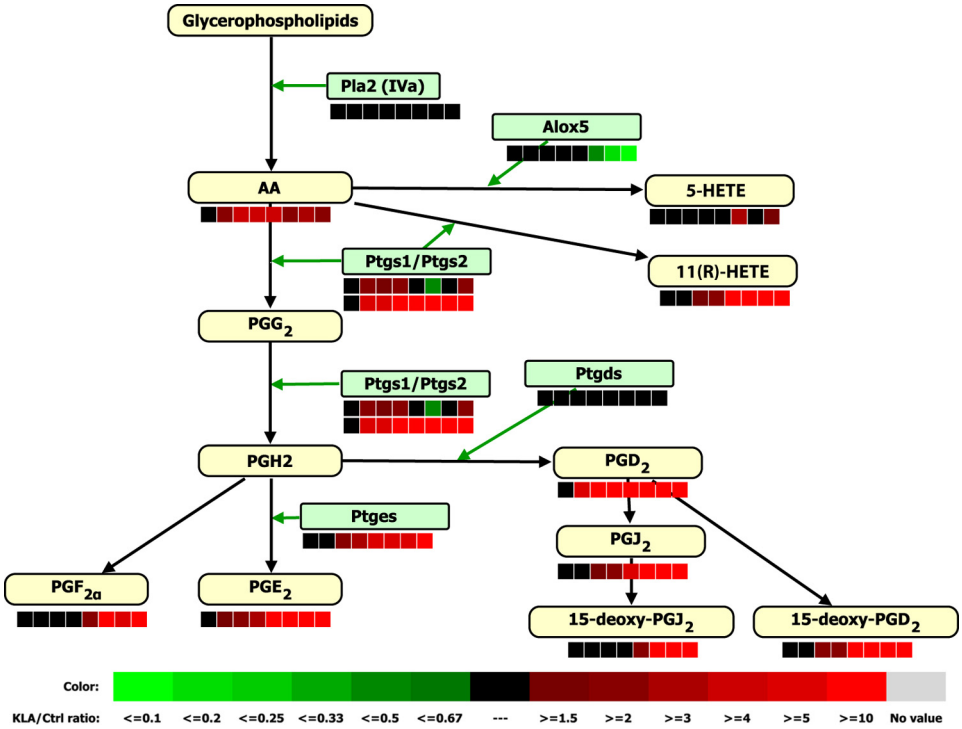

FIGURE 2. **Changes in eicosanoids in cell media and transcripts in response to KLA treatment of RAW cells.** *Green boxes* represent genes coding for enzymes that catalyze the indicated conversions, whereas *yellow boxes* represent lipid metabolites. The heat maps (see color key) below each lipid and gene represent the KLA/control (*KLA/Ctrl*) ratios at 0, 0.5, 1, 2, 4, 8, 12, and 24 h of treatment. Multiple gene isoforms are shown as heat maps that are stacked with the first isoform at the *top*. KLA/control ratio measurements for mRNAs and lipids were generated from averaging triplicate analyses of three separate RAW cell preparations. *5-HETE*, 5-hydroxyeicosatetraenoic acid; *11(R)HETE*, 11(*R*)-hydroxyeicosatetraenoicacid.

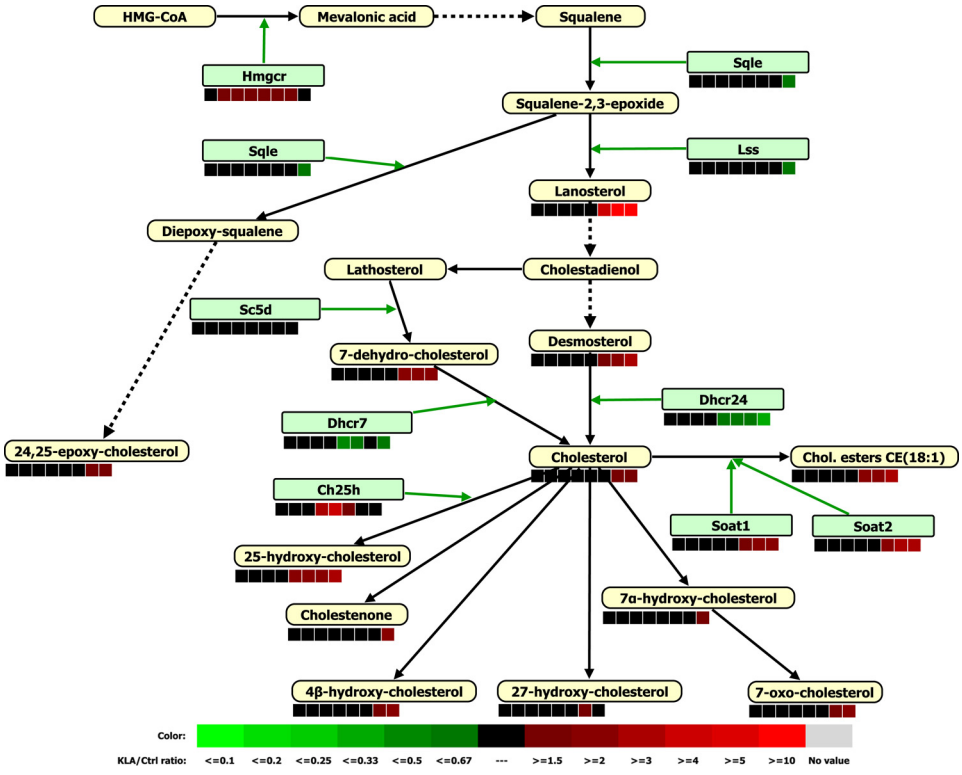

FIGURE 3. **Changes in sterols and transcripts in response to KLA treatment in RAW cells.** *Green boxes* represent genes coding for enzymes that catalyze the indicated conversion, whereas *yellow boxes* represent lipid metabolites. The heat maps below each lipid and gene represent the KLA/control (*KLA/Ctrl*) ratios at 0, 0.5, 1, 2, 4, 8, 12, and 24 h of treatment. Lipid and mRNA measurements were obtained as described in the legend for Fig. 2. *Chol. esters*, cholesteryl esters.

Some of the largest changes (10–20-fold) in lipid levels arising from KLA treatment of RAW cells occurred in cholesteryl esters containing saturated and monounsaturated fatty acyl groups. Smaller changes were detected in cholesteryl esters containing polyunsaturated fatty acyl substituents. These results suggested that saturated and monounsaturated cholesterol esters might accumulate as a result of increases in intracellular cholesterol levels arising from TLR4 activation. In agreement with this hypothesis, mRNAs encoding two cholesterol esterification enzymes (Soat1 and -2) increased 4–6-fold with KLA treatment. Two classes of prenols, dolichols and coenzyme Q, were increased 1.5–2-fold in both vehicle- and KLA-treated cells over the 24-h time course of the experiment; however, there were no accompanying alterations in mRNAs encoding prenol-metabolizing enzymes.

The correlation between various sterols and the genes for cholesterol biosynthesis is shown in supplemental Fig. 6, *A* and *B*. Consistent with the observations made above, cholesterol, its precursors, and its several derivatives co-vary with the mRNA of HMG CoA reductase (Hmgcr) and cholesterol 25-hydroxylase (Ch25h) (supplemental Table 2, Cluster 2). Cholesterol is made through two parallel pathways from lanosterol. As a result, its profile is a composite of the two effects; desmosterol increases from 0 to 24 h, as does 7-dehydro-cholesterol (supplemental Fig. 6*B*). However, Dhcr24 (supplemental Table 2, Cluster 3) in the first branch of cholesterol biosynthesis and Dhcr27 (supplemental Table 2, Cluster 1) in the second branch of cholesterol biosynthesis decrease over time (increasing only at the last time point at 24 h). As a net result, cholesterol exhibits a slightly non-monotonic time response, although the overall response shows an increase. We hypothesize that squalene-2,3-epoxide increases with time because both lanosterol and 24,25-epoxy-cholesterol increase,

although the mRNA levels of the corresponding genes/enzymes, lanosterol synthase (Lss) and squalene epoxidase (Sqle), respectively, decrease with time (supplemental Fig. 6*B*).

Sphingolipids—KLA treatment generated increases in almost every category of sphingolipid analyzed, including free sphingoid bases and their phosphates (*e.g.* sphingosine-1-phosphate), ceramides, sphingomyelins, and glycosphingolipids in RAW cells (supplemental Figs. 4, *C* and *D*, and 7). The earliest change occurred in sphinganine, which doubled within 2 h and remained elevated over most of the time course and was followed by increases in downstream metabolites, including *N*-acyl-sphinganines (dihydroceramides), after a lag of ~2–4 h. These increases were consistent with the induction of *de novo* sphingolipid biosynthesis because sphinganine and dihydroceramides are early intermediates in this pathway. Furthermore, the gene expression dataset revealed that mRNAs encoding two subunits of serine palmitoyltransferase (Sptlc1 and Sptlc2), the enzyme catalyzing the initial step of sphingolipid biosynthesis, were elevated in KLA-treated cells. A similar increase was observed for mRNAs encoding several ceramide synthases (CerS/Lass); however, the mRNA specifying CerS2, which produces very long-chain ceramides (C24:0 and C24:1), was not elevated, and the amounts of these acyl-chain length subspecies were the least affected (supplemental Fig. 4*C*). These results are readily observed in the correlation and data heat maps shown in supplemental Fig. 8, *A* and *B* where the largest cluster consists of 48 lipids and 7 genes including Sptlc1, Sptlc, Lass4, and Lass6 (supplemental Table 3, Cluster 2).

Sphingomyelins and glucosylceramides were increased with KLA treatment (1.5- and 3.5-fold, respectively). The elevation in sphingomyelins might reflect regulatory crosstalk between cholesterol metabolism and sphingolipid

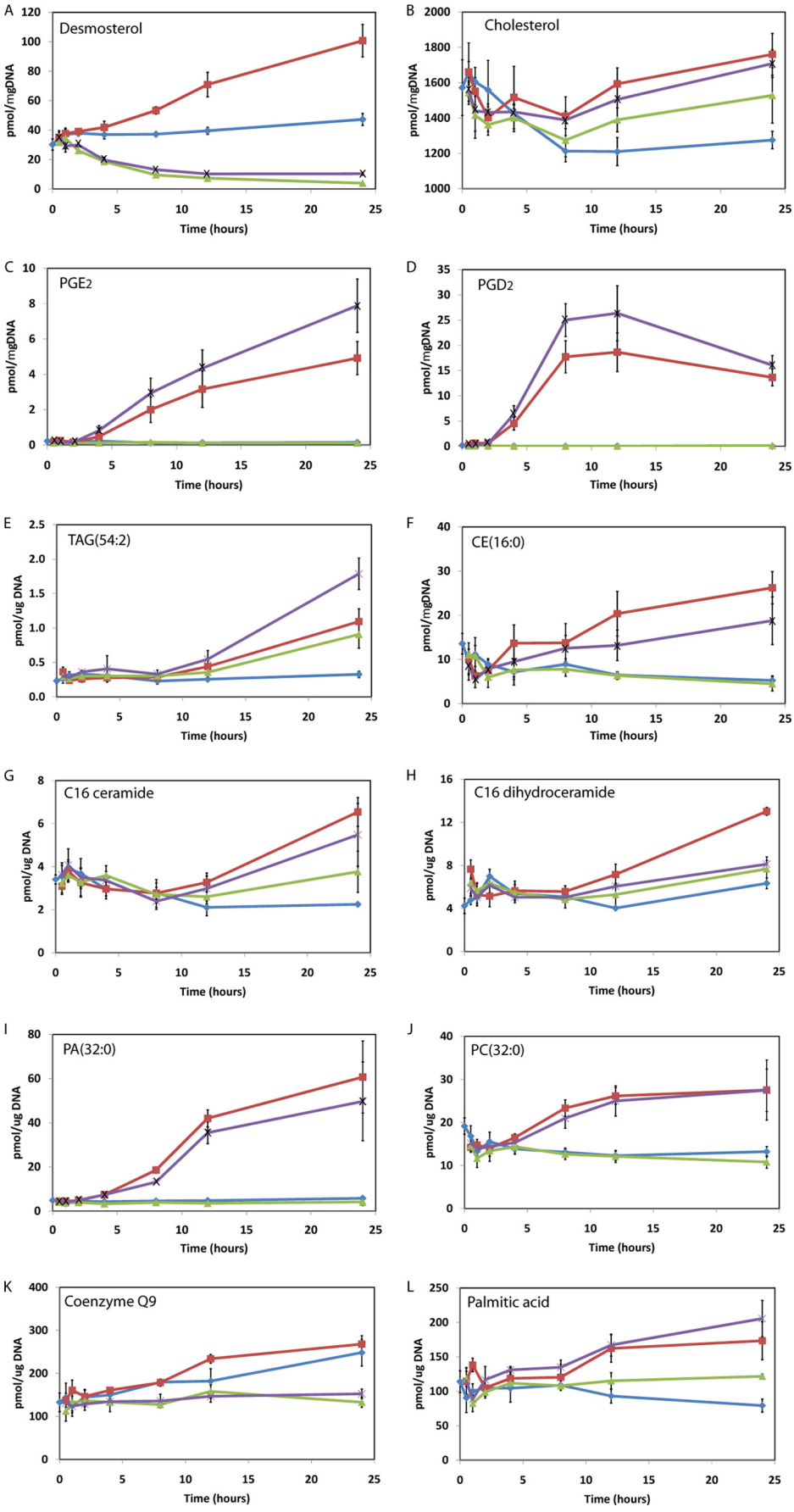

metabolism as oxysterols, which were found to be elevated by KLA (see above), alter sphingomyelin biosynthesis. The elevation in glucosylceramides was associated with an increase in the mRNA for the glycosyltransferase that makes these intermediates, UDP-glucose:ceramide glucosyltransferase. After treatment with KLA, RAW cells have substantially higher levels of galactosylceramides and sulfated galactosylceramides (sulfatides) (23). The increased production of sulfatides may be of biological significance as the presence of sulfated glycolipids on cells promotes their phagocytosis by macrophages (24), and sulfatides are one of the categories of endogenous lipids that bind to the CD1d cell surface receptor. Two other sphingolipid categories affected by KLA treatment and which have been widely implicated in cell signaling were the sphingoid base 1-phosphates (sphingosine 1-phosphate (S1P) and sphinganine-1-phosphate) and ceramide-1-phosphate (Cer1P). Sphingosine 1-phosphate and sphinganine-1-phosphate were elevated ~8-fold 12 h after KLA addition (supplemental Fig. 7).

Glycerophospholipids and Glycerolipids—The glycerophospholipid/glycerolipid categories are the largest quantitated, containing together several hundred analytes from over a thousand detected (supplemental Fig. *4D*). Total glycerophospholipids in KLA-treated samples remained roughly constant over the 24-h period, whereas control samples at 12 and 24 h had less total glycerophospholipid than the KLA-treated samples at these time points. Interestingly, significant changes in the phosphatidic acid and phosphatidylinositol classes were observed after 8–24 h of KLA stimulation. This trend was especially noticeable for the saturated and monounsaturated species in that the 32:0, 34:0, 34:1, 36:0, and 36:1 phosphatidic acid species increased by severalfold in response to the stimulus at the 24-h time point, suggesting that removal of the phosphate group from these lipids by phosphatidic acid phosphatases is responsible for the corresponding increases in the respective diacylglycerol species revealed by the glycerolipid analyses. The phosphatidylinositols exhibited a similar trend toward larger -fold increases for saturated species, whereas certain polyunsaturated species such as 38:4 phosphatidylinositol showed decreases of up to 50%. These results demonstrate that lipid second messengers and key metabolic intermediates (*i.e.* phosphatidic acid and diacylglycerols) are generated long after the initial presentation of the TLR4 ligand, which indicates that tonic intracellular signaling may continue throughout the 24-h period of stimulation.

Lipid Remodeling and Pharmacological Perturbation of Activated Macrophages by a Statin—We present herein an integrated view of lipid metabolism and remodeling that includes cross-talk between the six lipid categories discussed above as illustrated in the comprehensive overview of the major mammalian lipid categories and their interconnections shown in Fig. 1. Pathways to remodeling begin with the fatty acyl-CoA species. Careful measurements of acyl-CoAs after treatment with KLA show that although saturated CoA levels with the most chain lengths increase upon treatment, all the unsaturated CoA levels are decreased. Also, transcript levels of many desaturase genes are decreased in macrophages upon KLA treatment and are presumed to lead to reduced enzymatic levels for production of unsaturated acyl-CoAs. The temporal changes in the different lipid categories also support the remodeling of fatty acyls between glycerolipids, glycerophospholipids, sphingolipids, and sterol esters. The increased levels of palmitoyl CoA result in increased *de novo* synthesis of sphingolipids; the transcript level of serine palmitoyl transferase, the rate-limiting enzyme for the *de novo* synthesis of sphingolipids, is significantly elevated from the 4-h time point onward and peaks at the 18-h time point. The concomitant increase in the biosynthetic products desmosterol and lanosterol via acetyl CoA points to the involvement of sterol synthesis as well. These examples demonstrate the potential of a comprehensive integrated lipidomic/transcriptomic approach to understanding lipid metabolism.

Members of the statin class of drugs inhibit cholesterol biosynthesis by blocking the conversion of HMG-CoA into mevalonic acid. We reasoned that use of this selective inhibitor together with KLA would provide insight into how perturbations in one lipid biosynthetic pathway reverberate through the lipidome. To this end, RAW cells were treated over 24 h with and without KLA and in the presence or absence of 50 μM compactin, a commercially available statin. As expected, compactin blocked the KLA-stimulated increases in desmosterol (Fig. 4*A*), lanosterol, and 24,25-epoxy-cholesterol, which arise from the sterol biosynthetic pathway but had little or no effect on cholesterol levels (Fig. 4*B*) or 25-hydroxycholesterol levels, which can be derived from the uptake and degradation of cholesterol-rich lipoprotein particles in the cell medium and subsequent enzymatic hydroxylation. These relative changes are also visible in the data heat map for the combined data shown in supplemental Fig. 6*C*. In the large cluster, desmosterol and 24,25-epoxy-cholesterol are adjacent to each other, as are cholesterol and 25-hydroxycholesterol. Although these four lipids are in the same cluster, the two subgroups are far apart. Compactin treatment similarly slowed the increase in coenzyme Q that occurred with or without KLA stimulation, but in these experiments, levels of dolichol were unchanged under all conditions.

24,25-Epoxy-cholesterol and 25-hydroxycholesterol are ligands for the liver X receptor (LXR) (25). Activation of LXR by 24,25-epoxy-cholesterol is known to enhance the expression of genes encoding Abca1 and Abcg1, transporters that mediate cholesterol efflux, and to inhibit the expression of inflammatory response genes (26). These effects were confirmed by analyses of the transcriptomic and lipidomic datasets from the KLA/compactin experiments, which, for example, showed that Abcg1 mRNA levels correlated with those of 24,25-epoxy-cholesterol. That this response was due to LXR was confirmed in separate experiments carried out in bone marrow-derived macrophages from wild-type mice and knock-out mice lacking LXRα and LXRβ (data not shown).

FIGURE 4. **Time courses for selected lipids in RAW cells or media treated with KLA and/or compactin.** The legend is as follows: *blue diamond*, control; *red box*, KLA; *green triangle*, compactin; *purple X*, KLA + compactin. KLA/control ratio measurements for lipids were generated from the average analyses of three separate RAW cell preparations and are shown with standard errors.

An unexpected observation made in the compactin experiments was that inhibition of sterol biosynthesis caused an increase in the levels of two eicosanoids, PGD_2 and PGE_2, in response to KLA (Fig. 4, *C* and *D*). These increases correlated with elevations in the mRNAs encoding the respective biosynthetic enzymes of these eicosanoids, COX2 and PGE_2 synthase. This is also evident from the high correlation among these genes and lipids shown in supplemental Fig. 3, *A* and *B* (the *last three panels* in each figure). All four are in the same cluster. Studies in bone marrow-derived macrophages excluded roles for the LXRs in this apparent cross-talk between the sterol and eicosanoid pathways, suggesting the existence of a novel regulatory pathway involving transcription and signaling. Changes in multiple lipid molecular species of glycerophospholipids and cholesteryl esters were also observed as illustrated in Fig. 4, *F*, *I*, and *J*.

Novel Lipids—Using the protocols developed for mass spectrometric identification of lipids, we identified several novel lipids associated with macrophage cells. Several adrenic acids and elongated prostaglandins were found (27). Analysis of the phospholipid content of macrophage cell types (*i.e.* RAW, resident peritoneal macrophages, bone marrow-derived macrophages, and foam cells) has revealed dozens of rare or previously uncharacterized species of phospholipids, including phosphatidylthreonines, ether-linked phosphatidylinositols, phosphatidylserines, and glycerophosphatidic acids, as well as phosphatidylcholines and phosphatidylethanolamines containing very long polyunsaturated fatty acids (28). In preliminary studies, we have observed that KLA increased the 1-deoxysphingoid bases as well as their *N*-acyl-metabolites. Analysis of macrophage sterols revealed a novel role for a previously described lipid of unknown function. The oxysterol 25-hydroxycholesterol was initially described in the literature in 1974 (31, 32), and despite hundreds of studies in which this lipid was studied, a biological function remained undefined. Activated RAW macrophages were found to induce the cholesterol 25-hydroxylase gene and the synthesis of 25-hydroxycholesterol, which in turn was shown to regulate the production of immunoglobulin A by B cells of the adaptive immune system (29). Novel *N*-acyl-phosphatidylserine molecular species were detected in the phospholipids of mouse RAW cells (30). *N*-Acyl-phosphatidylserines may be the precursor of *N*-acyl-serine, a signaling lipid present in bovine brain, and it is possible that phospholipase D could cleave *N*-acyl-phosphatidylserine to generate *N*-acyl serine.

Conclusion—A living cell represents a highly integrated unit in which many thousands of lipid gene products must interact to ensure homeostasis in cell division, metabolism, and responsiveness. The switch from a reductionist to a constructionist approach in the scientific study of cells must begin with the identification of the many molecules that make up the cell. Recent studies along these lines have produced complete gene, mRNA, and protein parts lists, and here we add to these building blocks by reporting initial efforts to identify the many thousands of lipid molecular species that make up the mammalian macrophage. This number represents an underestimate as undoubtedly, not all lipids were extracted from the RAW cells by the organic solvents used and not all that were resolved were quantified by our analytical methods, so there will certainly be additional novel lipids present. Indeed, in the course of these studies, we discovered many lipid species not previously reported in macrophages including dihomoprostaglandins, ether-linked triglycerides, ether-linked phosphatidylinositol, ether-linked phosphatidylserine, phosphatidylthreonine, *N*-acyl phosphatidylserine, and deoxyceramides (data not shown).

The changes in lipid levels reported here were detected in multiple independent experiments, suggesting that each has a biological meaning. In some cases, such as for eicosanoids, the consequences for macrophage function and inflammation are well defined, whereas for a majority of the other lipid changes, determining the effects and physiological significance will require future investigations. We have presented herein a comprehensive picture of the dynamics of lipid metabolism in the functioning of a mammalian cell using a systems biology approach (see supplemental Fig. 9 for pathway map). This is the first quantitative approach toward the complete characterization of the lipidome of a mammalian cell and its regulation during immunological stimulation and pharmacological inhibition in a model for disease processes.

Acknowledgments—We thank additional LIPID MAPS investigators Dr. Michael S. VanNieuwenhze (Indiana University), Dr. Stephen H. White (University of California, Irvine), Dr. Nicholas Winograd (Penn State University), and Dr. Joseph L. Witztum (University of California, San Diego), who actively participate in the LIPID MAPS initiative, and additional LIPID MAPS personnel Jeremy C. Allegood, Aaron Armando, Michelle D. Armstrong, Robert Byrnes, Christopher A. Haynes, Pavlina T. Ivanova, Samuel Kelly, Reza Kordestani, Sean Li, Holly A. Lincoln, and Rebecca Shaner for technical assistance and Masada Disenhouse for administrative assistance.

REFERENCES

1. Gilman, A. G., Simon, M. I., Bourne, H. R., Harris, B. A., Long, R., Ross, E. M., Stull, J. T., Taussig, R., Bourne, H. R., Arkin, A. P., Cobb, M. H., Cyster, J. G., Devreotes, P. N., Ferrell, J. E., Fruman, D., Gold, M., Weiss, A., Stull, J. T., Berridge, M. J., Cantley, L. C., Catterall, W. A., Coughlin, S. R., Olson, E. N., Smith, T. F., Brugge, J. S., Botstein, D., Dixon, J. E., Hunter, T., Lefkowitz, R. J., Pawson, A. J., Sternberg, P. W., Varmus, H., Subramaniam, S., Sinkovits, R. S., Li, J., Mock, D., Ning, Y., Saunders, B., Sternweis, P. C., Hilgemann, D., Scheuermann, R. H., DeCamp, D., Hsueh, R., Lin, K. M., Ni, Y., Seaman, W. E., Simpson, P. C., O'Connell, T. D., Roach, T., Simon, M. I., Choi, S., Eversole-Cire, P., Fraser, I., Mumby, M. C., Zhao, Y., Brekken, D., Shu, H., Meyer, T., Chandy, G., Heo, W. D., Liou, J., O'Rourke, N., Verghese, M., Mumby, S. M., Han, H., Brown, H. A., Forrester, J. S., Ivanova, P., Milne, S. B., Casey, P. J., Harden, T. K., Arkin, A. P., Doyle, J., Gray, M. L., Meyer, T., Michnick, S., Schmidt, M. A., Toner, M., Tsien, R. Y., Natarajan, M., Ranganathan, R., and Sambrano, G. R. (2002) *Nature* **420,** 703–706
2. Papin, J. A., Hunter, T., Palsson, B. O., and Subramaniam, S. (2005) *Nat. Rev. Mol. Cell Biol.* **6,** 99–111
3. Dennis, E. A. (2009) *Proc. Natl. Acad. Sci. U.S.A.* **106,** 2089–2090
4. Murphy, R. C., Fiedler, J., and Hevko, J. (2001) *Chem. Rev.* **101,** 479–526
5. Ivanova, P. T., Cerda, B. A., Horn, D. M., Cohen, J. S., McLafferty, F. W., and Brown, H. A. (2001) *Proc. Natl. Acad. Sci. U.S.A.* **98,** 7152–7157
6. Dennis, E. A. (2005) in *Functional Lipidomics* (Feng, L., and Prestwich, G., eds.) pp. 1–15, CRC Press, New York
7. Wenk, M. R. (2005) *Nat. Rev. Drug Discov.* **4,** 594–610
8. van Meer, G. (2005) *EMBO J.* **24,** 3159–3165
9. Kim, J. K. (2006) *Cell Metab.* **4,** 417–419
10. Werner, S. L., Barken, D., and Hoffmann, A. (2005) *Science* **309,**

1857–1861
11. Wu, H. M., Jin, M., and Marsh, C. B. (2005) *Am. J. Physiol. Lung Cell. Mol. Physiol.* **288,** L585-L595
12. Fahy, E., Subramaniam, S., Murphy, R. C., Nishijima, M., Raetz, C. R., Shimizu, T., Spener, F., van Meer, G., Wakelam, M. J., and Dennis, E. A. (2009) *J. Lipid Res.* **50,** (suppl) S9–S14
13. Fahy, E., Subramaniam, S., Brown, H. A., Glass, C. K., Merrill, A. H., Jr., Murphy, R. C., Raetz, C. R., Russell, D. W., Seyama, Y., Shaw, W., Shimizu, T., Spener, F., van Meer, G., VanNieuwenhze, M. S., White, S. H., Witztum, J. L., and Dennis, E. A. (2005) *J. Lipid Res.* **46,** 839–861
14. Brown, H. A. (2007) *Methods Enzymol.* **432,** 1–400
15. Raetz, C. R., Garrett, T. A., Reynolds, C. M., Shaw, W. A., Moore, J. D., Smith, D. C., Jr., Ribeiro, A. A., Murphy, R. C., Ulevitch, R. J., Fearns, C., Reichart, D., Glass, C. K., Benner, C., Subramaniam, S., Harkewicz, R., Bowers-Gentry, R. C., Buczynski, M. W., Cooper, J. A., Deems, R. A., and Dennis, E. A. (2006) *J. Lipid Res.* **47,** 1097–1111
16. Park, B. S., Song, D. H., Kim, H. M., Choi, B. S., Lee, H., and Lee, J. O. (2009) *Nature* **458,** 1191–1195
17. Byrnes, R. W., Fahy, E., and Subramaniam, S. (2007) *J. Assoc. Laboratory Automation* **12,** 230–238
18. Buczynski, M. W., Stephens, D. L., Bowers-Gentry, R. C., Grkovich, A., Deems, R. A., and Dennis, E. A. (2007) *J. Biol. Chem.* **282,** 22834–22847
19. Gupta, S., Maurya, M. R., Stephens, D. L., Dennis, E. A., and Subramaniam, S. (2009) *Biophysical Journal* **96,** 4542–4551
20. Buczynski, M. W., Dumlao, D. S., and Dennis, E. A. (2009) *J. Lipid Res.* **50,** 1015–1038
21. Flowers, M. T., and Ntambi, J. M. (2008) *Curr. Opin. Lipidol.* **19,** 248–256
22. Brown, M. S., and Goldstein, J. L. (2009) *J. Lipid Res.* **50,** S15-S27
23. Shaner, R. L., Allegood, J. C., Park, H., Wang, E., Kelly, S., Haynes, C. A., Sullards, M. C., and Merrill, A. H., Jr. (2009) *J. Lipid Res.* **50,** 1692–1707
24. Popovic, Z. V., Sandhoff, R., Sijmonsma, T. P., Kaden, S., Jennemann, R., Kiss, E., Tone, E., Autschbach, F., Platt, N., Malle, E., and Gröne, H. J. (2007) *J. Immunol.* **179,** 6770–6782
25. Janowski, B. A., Willy, P. J., Devi, T. R., Falck, J. R., and Mangelsdorf, D. J. (1996) *Nature* **383,** 728–731
26. Ghisletti, S., Huang, W., Ogawa, S., Pascual, G., Lin, M. E., Willson, T. M., Rosenfeld, M. G., and Glass, C. K. (2007) *Mol. Cell* **25,** 57–70
27. Harkewicz, R., Fahy, E., Andreyev, A., and Dennis, E. A. (2007) *J. Biol. Chem.* **282,** 2899–2910
28. Ivanova, P. T., Milne, S. B., and Brown, H. A. (2010) *J. Lipid Res.* **51,** 1581–1590
29. Bauman, D. R., Bitmansour, A. D., McDonald, J. G., Thompson, B. M., Liang, G., and Russell, D. W. (2009) *Proc. Natl. Acad. Sci. U.S.A.* **106,** 16764–16769
30. Guan, Z., Li, S., Smith, D. C., Shaw, W. A., and Raetz, C. R. (2007) *Biochemistry* **46,** 14500–14513
31. Brown, M. S., and Goldstein, J. L. (1974) *J. Biol. Chem.* **249,** 7306–7314
32. Kandutsch, A. A., and Chen, H. W. (1974) *J. Biol. Chem.* **249,** 6057–6061